Wide-angle near infrared polarizer with extremely high extinction ratio

X. L. Liu, B. Zhao, and Z. M. Zhang*

George W. Woodruff School of Mechanical Engineering, Georgia Institute of Technology, Atlanta, GA 30332, USA

**zhuomin.zhang@me.gatech.edu*

Abstract: An infrared polarizer is designed with a predicted extremely high extinction ratio exceeding 3×10^{16} and transmittance higher than 89% for one polarization in the wavelength region from 1.6 to 2.3 μm. Moreover, the performance does not start to deteriorate until 60° tilting angle. The wide-angle high transmission is attributed to the excitation of magnetic polaritons and suitable LC circuit models, which could predict the resonance wavelengths quantitatively, are developed to better understand the underlying mechanisms. The proposed structure can be tuned by controlling the geometrical parameters for different potential applications such as polarizers, beamsplitters, filters, and transparent electrodes.

OCIS codes: (230.5440) Polarization-selective devices; (240.5420) Polaritons; (050.2770) Gratings; (120.7000) Transmission.

References and links

1. Y. T. Pang, G. W. Meng, Q. Fang, and L. D. Zhang, "Silver nanowire array infrared polarizers," Nanotechnology **14**(1), 20–24 (2003).
2. L. Zhou and W. Liu, "Broadband polarizing beam splitter with an embedded metal-wire nanograting," Opt. Lett. **30**(12), 1434–1436 (2005).
3. Y.-B. Chen, B. J. Lee, and Z. M. Zhang, "Infrared radiative properties of submicron metallic slit arrays," J. Heat Transf.-Trans. ASME **130**(8), 082404 (2008).
4. Y. Ekinci, H. H. Solak, C. David, and H. Sigg, "Bilayer Al wire-grids as broadband and high-performance polarizers," Opt. Express **14**(6), 2323–2334 (2006), http://www.opticsinfobase.org/oe/abstract.cfm?uri=OE-14-6-2323.
5. S.-W. Ahn, K.-D. Lee, J.-S. Kim, S. H. Kim, J.-D. Park, S.-H. Lee, and P.-W. Yoon, "Fabrication of a 50 nm half-pitch wire grid polarizer using nanoimprint lithography," Nanotechnology **16**(9), 1874–1877 (2005).
6. L. Chen, J. J. Wang, F. Walters, X. Deng, M. Buonanno, S. Tai, and X. Liu, "Large flexible nanowire grid visible polarizer made by nanoimprint lithography," Appl. Phys. Lett. **90**(6), 063111 (2007).
7. F. Miyamaru and M. Hangyo, "Anomalous terahertz transmission through double-layer metal hole arrays by coupling of surface plasmon polaritons," Phys. Rev. B **71**(16), 165408 (2005).
8. C. Cheng, J. Chen, D.-J. Shi, Q.-Y. Wu, F.-F. Ren, J. Xu, Y.-X. Fan, J. Ding, and H.-T. Wang, "Physical mechanism of extraordinary electromagnetic transmission in dual-metallic grating structures," Phys. Rev. B **78**(7), 075406 (2008).
9. L. P. Wang and Z. M. Zhang, "Effect of magnetic polaritons on the radiative properties of double-layer nanoslit arrays," J. Opt. Soc. Am. B **27**(12), 2595–2604 (2010).
10. H. B. Chan, Z. Marcet, K. Woo, D. B. Tanner, D. W. Carr, J. E. Bower, R. A. Cirelli, E. Ferry, F. Klemens, J. Miner, C. S. Pai, and J. A. Taylor, "Optical transmission through double-layer metallic subwavelength slit arrays," Opt. Lett. **31**(4), 516–518 (2006).
11. Z. Y. Yang and Y. F. Lu, "Broadband nanowire-grid polarizers in ultraviolet-visible-near-infrared regions," Opt. Express **15**(15), 9510–9519 (2007), http://www.opticsinfobase.org/oe/abstract.cfm?uri=oe-15-15-9510.
12. J. J. Peltzer, P. D. Flammer, T. E. Furtak, R. T. Collins, and R. E. Hollingsworth, "Ultra-high extinction ratio micropolarizers using plasmonic lenses," Opt. Express **19**(19), 18072–18079 (2011), http://www.opticsinfobase.org/oe/abstract.cfm?uri=oe-19-19-18072.
13. B. J. Lee, Y.-B. Chen, and Z. M. Zhang, "Transmission enhancement through nanoscale metallic slit arrays from the visible to mid-infrared," J. Comput. Theor. Nanosci. **5**, 201–213 (2008).
14. M. F. Modest, *Radiative Heat Transfer,* 2nd Ed. (Academic Press, 2003).
15. E. D. Palik, ed., *Handbook of Optical Constants of Solids*, Vol. 1 (Academic Press, 1998).
16. Z. M. Zhang, T. R. Gentile, A. L. Migdall, and R. U. Datla, "Transmittance measurements for filters of optical density between one and ten," Appl. Opt. **36**(34), 8889–8895 (1997).
17. G. Kang, Y. Fang, I. Vartiainen, Q. Tan, and Y. Wang, "Achromatic polarization splitting effect of metallic gratings with sub-50 nm wide slits," Appl. Phys. Lett. **101**(21), 211104 (2012).

#186509 - $15.00 USD Received 6 Mar 2013; revised 13 Apr 2013; accepted 14 Apr 2013; published 23 Apr 2013

18. W.-D. Li, J. Hu, and S. Y. Chou, "Extraordinary light transmission through opaque thin metal film with subwavelength holes blocked by metal disks," Opt. Express **19**(21), 21098–21108 (2011), http://www.opticsinfobase.org/oe/abstract.cfm?uri=oe-19-21-21098.
19. Y. Zhao, M. A. Belkin, and A. Alù, "Twisted optical metamaterials for planarized ultrathin broadband circular polarizers," Nat. Commun. **3**, 870 (2012).
20. S. Xie, H. Li, S. Fu, H. Xu, X. Zhou, and Z. Liu, "The extraordinary optical transmission through double-layer gold slit arrays," Opt. Commun. **283**(20), 4017–4024 (2010).
21. Z. Ye, Y. Peng, T. Zhai, Y. Zhou, and D. Liu, "Surface plasmon-mediated transmission in double-layer metallic grating polarizers," J. Opt. Soc. Am. B **28**(3), 502–507 (2011).
22. L. Y. Deng, J. H. Teng, L. Zhang, Q. Y. Wu, H. Liu, X. H. Zhang, and S. J. Chua, "Extremely high extinction ratio terahertz broadband polarizer using bilayer subwavelength metal wire-grid structure," Appl. Phys. Lett. **101**(1), 011101 (2012).
23. X.-R. Huang and R.-W. Peng, "General mechanism involved in subwavelength optics of conducting microstructures: charge-oscillation-induced light emission and interference," J. Opt. Soc. Am. A **27**(4), 718–729 (2010).
24. L. P. Wang and Z. M. Zhang, "Wavelength-selective and diffuse emitter enhanced by magnetic polaritons for thermophotovoltaics," Appl. Phys. Lett. **100**(6), 063902 (2012).
25. Z. M. Zhang, *Nano/Microscale Heat Transfer* (McGraw-Hill, 2007).
26. B. Zhao, L. P. Wang, Y. Shuai, and Z. M. Zhang, "Thermophotovoltaic emitters based on a two-dimensional grating/thin-film nanostructure," Int. J. Heat Mass Transfer (submitted to) (2013).
27. Y. Cui and S. He, "Enhancing extraordinary transmission of light through a metallic nanoslit with a nanocavity antenna," Opt. Lett. **34**(1), 16–18 (2009).

1. Introduction

Polarizers play an important role in optical devices and systems, such as the Faraday isolators, modulators, fiber-optic networks, as well as imaging and laser systems. High-efficiency near-infrared polarizers are especially important for laser systems and optical communications. Compared with conventional bulky polarizers, such as calcite prisms and pile of plates, which are difficult to integrate with other components, wire-grid polarizers can be used to produce compact and integrated optical devices. Anodization and elctrodeposition [1], e-beam lithography [2, 3], interference lithography [4], and nanoimprint lithography [5, 6] have already been used to fabricate wire-grid polarizers applicable to the near-infrared region. The performance of a polarizer can be characterized by a high transmittance for one polarization and very low transmittance for another polarization. Appropriate lateral shift is suggested to enhance the transmission of double-layer periodic gratings at certain wavelength region [4, 7–10]. Chan et al. [10] experimentally demonstrated an extraordinary transmission for transverse magnetic (TM) waves in a double-layer grating nanostructure. Yang and Lu [11] designed an extra-broadband polarizer by incorporating dual-layer aluminum grating on both sides of the CaF_2 substrate. This structure was predicted to have an extinction ratio, the ratio of transmittance for TM waves to that of TE (electric field is perpendicular to the incidence plane) waves, exceeding 10^7 and transmission over 64% in the wavelength (λ) region from 0.3 to 5 μm. The highest extinction ratio was predicted to be 10^9 at $\lambda = 5$ μm [11]. Peltzer et al. [12] designed and fabricated a near-infrared polarizer with a theoretically predicted extinction ratio as high as 10^{11} in a narrow spectral region.

In this work, a design of a broadband polarizer with high transmittance (near 90%) and extremely high extinction ratio (exceeding 10^{16}) for 1.6 μm < λ < 2.3 μm is proposed. The device can also act as a polarization beamsplitter. Furthermore, the performance does not degrade until a tilting angle of 60° is reached. Magnetic (plasmon) polaritons (MPs) are used to elucidate the extraordinary transmission in a relatively broad spectral region.

2. High transmission and extinction ratio

The structure proposed here is based on a one-dimensional (1D) double-layer structure, which is periodic along the x direction and extends to infinity in the y direction, as shown in Fig. 1(a). A thin SiO_2 (glass) spacer is sandwiched between two identical silver gratings, which are shifted laterally by half the period. In other words, the centerlines of the ridges in the top grating coincide with those of the slits in the bottom grating. The structure is characterized with a base set of parameters given in the following: the period P = 500 nm, spacer thickness t_s = 30 nm, Ag grating thickness t_m = 400 nm, and slit width W_g = 150 nm. Radiation is

#186509 - $15.00 USD Received 6 Mar 2013; revised 13 Apr 2013; accepted 14 Apr 2013; published 23 Apr 2013

incident from air at an incidence angle of θ_i. The analysis is based on finite-difference time-domain (FDTD) method using a commercial package (Lumerical Solutions, Inc.) and the rigorous coupled-wave analysis (RCWA) algorithm [9, 13].

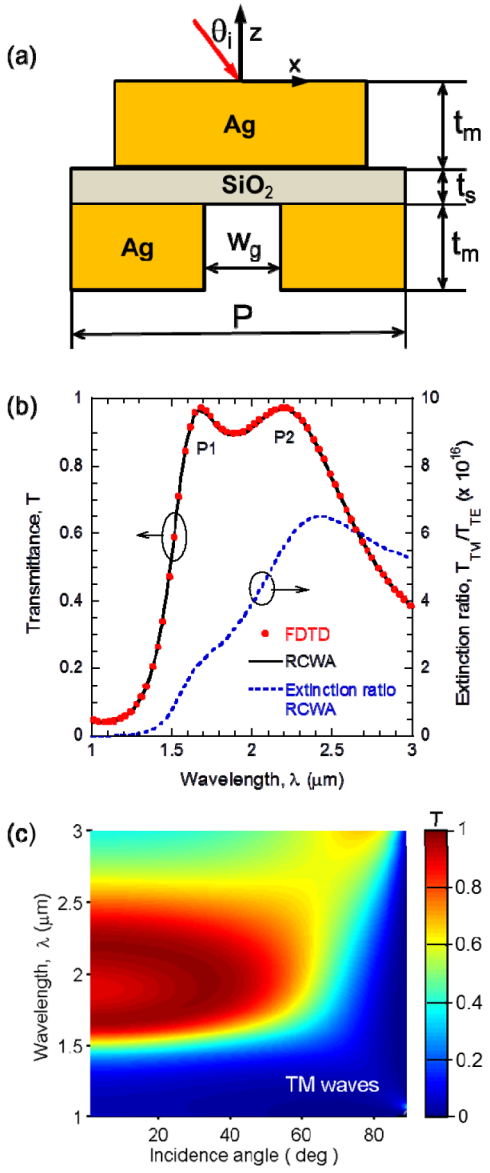

Fig. 1. The proposed nanostructure and its performance as an IR polarizer: (a) Schematic of a period of the double-layer grating; (b) Spectral transmittance for TM waves and the extinction ratio at normal incidence; (c) Contour plot of the transmittance as a function of the wavelength and angle of incidence for TM waves. The parameters used for the calculation are P = 500 nm, t_m = 400 nm, t_s = 30 nm, and W_g = 150 nm.

The dielectric function of Ag as a function of the angular frequency ω is obtained using the Drude model: $\varepsilon_{Ag}(\omega) = \varepsilon_\infty - \omega_p^2 / (\omega^2 - i\gamma\omega)$ with a scattering rate $\gamma = 2.7\times10^{13}$ rad/s, plasma frequency $\omega_p = 1.39\times10^{16}$ rad/s, and a high-frequency constant $\varepsilon_\infty = 3.4$ [14]. For

#186509 - $15.00 USD Received 6 Mar 2013; revised 13 Apr 2013; accepted 14 Apr 2013; published 23 Apr 2013

SiO_2, the refraction index is taken as 1.43 with negligible loss in the considered wavelength region from 1 to 3 μm [15].

Figure 1(b) shows the calculated transmittance for TM waves at normal incidence using both FDTD and RCWA methods, which give essentially the same results, as well as the extinction ratio calculated with RCWA. Transmittance higher than 89% is predicted in a broad wavelength region from 1.6 to 2.3 μm. The extinction ratio is surprisingly high, exceeding 3×10^{16} across the aforementioned spectral region with high transmittance. For a homogeneous Ag thin film, the normal transmittance is lower than 10^{-16} with a film thickness of 400 nm and lower than 10^{-20} with a thickness of 500 nm. Therefore, it is not surprising why the transmittance of the proposed structure is so low for TE waves. Due to the extremely low transmittance values for TE waves, results obtained from the FDTD simulation tend to fluctuate and are not reliable because of the numerical errors. However, the RCWA algorithm uses double-precision data type. The accuracy of the RCWA model is limited only by the number of diffraction orders used. By increasing the number of diffraction order, convergence can be reached even with ultralow transmittance values. The transmittance for a homogeneous film predicted using RCWA is essentially the same as that calculated from thin-film topics at extremely low transmittance (down to 10^{-30}). It should be noted that the extremely high extinction ratio will be important for devices or systems that require ultrahigh polarization purity such as high power laser systems and high contrast modulators. If used in Faraday isolators, the proposed polarizer will help to suppress the back light completely, given that transmittance down to 10^{-11} is still measurable [16]. The transmittance spectra are featured with two peaks labeled as P1 and P2. Note that P1 is at $\lambda = 1.69$ μm with $T = 97.3\%$ and P2 is at $\lambda = 2.10$ μm with $T = 97.4\%$. Moreover, in the high transmission regime, the average reflectance for TM waves is only 3.6% (the maximum value is about 8.1%). On the other hand, the reflectance for TE waves is greater than 99.5% in the aforementioned region. Therefore, the proposed structure can also be used as a polarization-selective beamsplitter [17].

Figure 1(c) displays the transmittance contour as a function of the wavelength and incidence angle. Note that the plane of incidence is always perpendicular to the *y*-axis to avoid conical refraction when depolarization can occur [13]. It can be seen that the transmittance is still high until the incidence angle exceeds 60°. It should be noted that the transmittance for TE waves (not shown) remains to be extremely low at oblique incidence. That means the polarizer has a large angle tolerance, which makes it useful not only for well collimated beams, but also for diverging and converging beams. The two peaks approach each other with increasing incident angles and finally merge together when the incidence angle exceeds 25°.

For practical applications, the proposed structure may be fabricated onto a suitable substrate material such as SiO_2 or CaF_2. If the slit region is filled with a dielectric rather than air, the fabrication process will not be too difficult because similar structures have been fabricated by others [10, 12, 18, 19]. High performance is still expected when the slit region is filled with a dielectric material, although some tuning of the parameters is necessary for wavelength selection. Moreover, the dielectric in the silt region (different from the material used as the spacer) could be removed by wet etching in the final step if necessary. Attention is now turned to the underlying mechanisms that give rise to the high and broadband transmission for TM waves.

3. *LC* circuit models and magnetic polaritons

Extraordinary transmission through double-layer gratings with or without lateral shift has been investigated by many researchers [4, 8, 11, 20–22]. Different mechanisms were used to explain this phenomenon, such as coupled surface plasmons, waveguide modes, or Fabry-Perot resonances. Recently, Huang and Peng [23] put forward a general charge-oscillation theory to explain the extraordinary transmission through various sub-wavelength decorated metallic structures. Nonetheless, few of them could predict the location of the transmission

#186509 - $15.00 USD Received 6 Mar 2013; revised 13 Apr 2013; accepted 14 Apr 2013; published 23 Apr 2013

peak quantitatively. Here, the two transmission peaks are attributed to magnetic polaritons (MPs) which refer to the coupling between the external electromagnetic waves and the induced current loop in a micro/nanostructure [9, 24]. Two simple inductor-capacitor (LC) circuit models are developed after carefully analyzing the magnetic field distribution and current density vectors in the near-field regime to quantitatively predict the locations of the transmission peaks P1 and P2, respectively, as shown in Fig. 2.

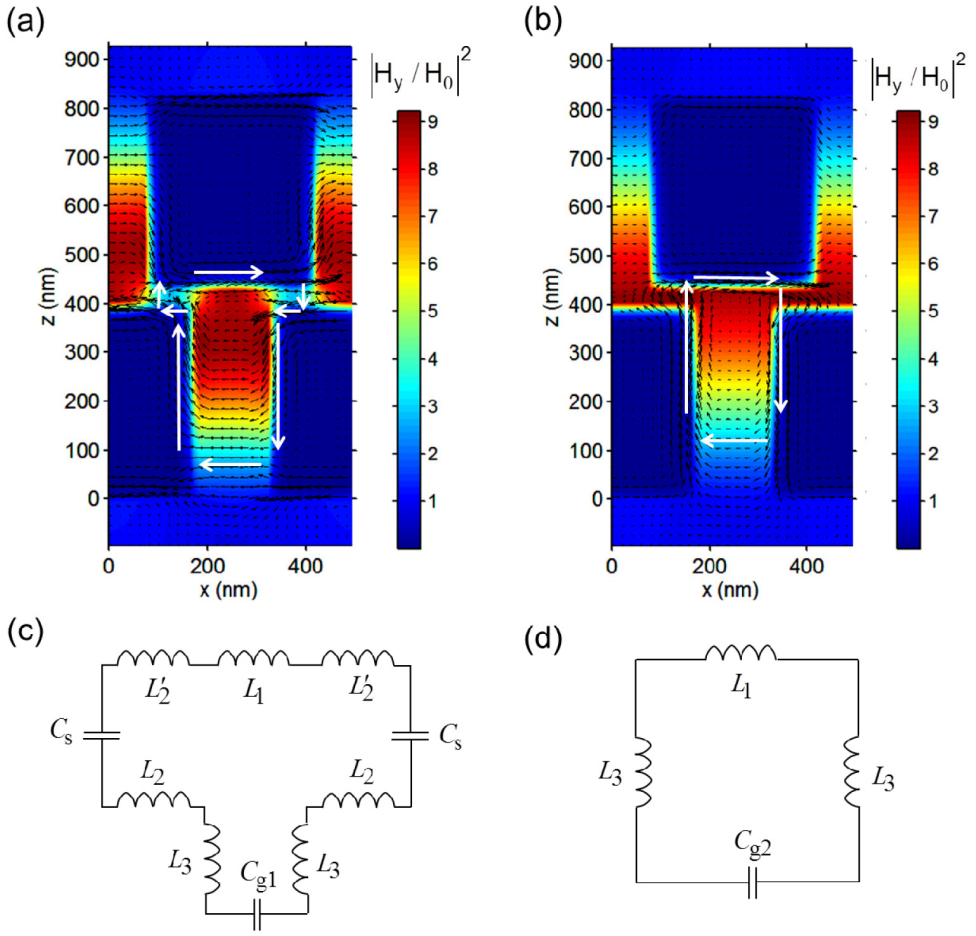

Fig. 2. The enhancement of the magnetic field and current loop when the MPs are excited and the simple LC circuit models: (a,b) Contour plots of the dimensionless field distribution $|H_y / H_0|^2$ for P1 and P2, respectively. The arrows indicate the directions of the current flow; (c,d) LC models for P1 and P2, respectively, based on the magnetic field and current density distributions.

For the first peak (P1), the dimensionless field distribution is shown in Fig. 2(a) with color denoting $|H_y / H_0|^2$ and arrows representing the current density vectors. Here, H_0 is the amplitude of the magnetic field for the incident wave. There exists strong field enhancement in the slit and the SiO_2 spacer region but not in the overlapping area between the top and bottom gratings. Following the current density vectors distribution, a LC model shown in Fig. 2(c) is developed to predict the resonance wavelength for P1. Note that the field distributions in the top and bottom slits are almost the same due to the structure symmetry, so that only one LC circuit either in the top or bottom slit region is needed to predict the resonance wavelength

#186509 - $15.00 USD Received 6 Mar 2013; revised 13 Apr 2013; accepted 14 Apr 2013; published 23 Apr 2013

(or frequency). The simple LC circuit model assumes that MPs are localized without coupling to each other. The inductances are given as follows:

$$L_1 = L_{e,1} = \frac{W_g}{\varepsilon_0 \omega_p^2 \delta l} \tag{1}$$

$$L_2' = L_2 = L_{e,2} + L_{m,2} = \frac{(P - 2W_g)}{4\varepsilon_0 \omega_p^2 \delta l} + \frac{\mu_0 (P - 2W_g) t_s}{8l} \tag{2}$$

$$L_3 = L_{e,3} + L_{m,3} = \frac{t_m}{\varepsilon_0 \omega_p^2 \delta l} + \frac{\mu_0 W_g t_m}{2l} \tag{3}$$

where μ_0 and ε_0 are the permeability and permittivity of vacuum, respectively, and l is the structure thickness in the y direction. Here, $L_{e,1}$, $L_{e,2}$, and $L_{e,3}$ are the kinetic inductances that account for the contribution of drifting electrons, while $L_{m,2}$ and $L_{m,3}$ are the mutual inductances between parallel plates [9, 24]. It is assumed that all induced electric current in the metal flows within a penetration depth defined as $\delta = \lambda / 4\pi\kappa$, where κ is the extinction coefficient of Ag [25]. In Fig. 2(c), C_{g1} and C_s are the parallel-plate capacitances of the gap (slit) and spacer, respectively, and are given as

$$C_{g1} = \frac{c_1 \varepsilon_0 t_m l}{W_g} \quad \text{and} \quad C_s = \frac{c_2 \varepsilon_0 \varepsilon_d (P - 2W_g) l}{4t_s} \tag{4}$$

where ε_d is the permittivity of SiO_2. The coefficients c_1 and c_2 take into account the nonuniform charge distribution and are often treated as adjusting parameters [9, 24, 26]. In the present study, good agreement between the resonance wavelengths calculated by the rigorous numerical solutions and the LC model are obtained using $c_1 = c_2 = 0.6$. It can be seen from Fig. 2(a) that the field and current density in the slit region are nonuniform. The charge distribution is also nonuniform since charges tend to accumulate around the corner. Similarly, the field and charge distributions are nonuniform in the overlapping area between the top and bottom gratings, although not shown in Fig. 2(a). The MP resonance condition in this LC circuit can be determined by zeroing the total impedance, and then the (angular) resonant frequency is obtained as follows.

$$\omega_{p1} = \sqrt{\left(\frac{2}{C_s} + \frac{1}{C_{g1}}\right) \frac{1}{L_1 + 2L_2' + 2L_2 + 2L_3}} \tag{5}$$

For the second peak (P2), the dimensionless field distribution is shown in Fig. 2(b), which is featured with the strong field confinement in the whole spacer and slit region. The current density in the spacer between the region where the top and bottom gratings overlap is so large that the impedance could be neglected. Consequently, it appears as if the side wall of the bottom grating is extended all the way to the top grating, as illustrated in the LC model shown in Fig. 2(d). Here, the slit or gap capacitance C_{g2} considering this extending effect is given as

$$C_{g2} = \frac{c_3 \varepsilon_0 t_m l}{W_g} + \frac{c_4 \varepsilon_0 \varepsilon_d t_s l}{W_g} \tag{6}$$

Similar to c_1 and c_2 in the previous model, c_3 and c_4 are introduced to account for the nonuniform charge distribution and are taken as adjustable parameters. Good agreement between the resonance wavelengths predicted by the LC model and the rigorous solutions is obtained with $c_3 = 0.3$ and $c_4 = 1$. The reason that c_3 is much smaller than c_1 can be explained

#186509 - $15.00 USD Received 6 Mar 2013; revised 13 Apr 2013; accepted 14 Apr 2013; published 23 Apr 2013

as due to the fact that the electromagnetic fields are confined mainly in the region close to the spacer when P2 is excited. Inside the spacer region, however, the field is greatly enhanced and almost uniformly distributed so that c_4 should be close to 1. The resonance frequency for P2 of this circuit is given as

$$\omega_{p2} = \sqrt{\frac{1}{C_{g2}(L_1 + 2L_3)}} \tag{7}$$

The resonance wavelengths predicted by the LC models are 1.674 μm (P1) and 2.298 μm (P2), which agree well with the values of 1.685 μm (P1) and 2.195 μm (P2) obtained by numerical simulations. It should be noted that the maximum absorptance in the high transmittance band is only 3.2%; therefore, the strong field confinement mainly helps light to penetrate through this structure. The LC models not only provide a physical interpretation of the extraordinary transmission, but also allow quantitative predictions of the geometric effect on the resonance condition as discussed in the following.

4. Performance tunability

It is important to understand the dependence of transmittance on the various geometric parameters in order to design polarizers suitable for specific applications. This is done by varying some parameters while fixing the rest as in the base set mentioned before. The results are shown in Fig. 3, where the color contours are from the full-wave numerical simulations and the dashed lines are from the LC circuit models. The circle and triangle marks indicate the excitation of P1 and P2, respectively, with the base set of parameters. When the Ag grating thickness t_m increases, the high transmittance region will redshift (i.e., toward longer wavelengths), as shown in Fig. 3(a). Similar trends have been observed earlier [8]. The peak wavelengths can be well predicted by the LC models. The redshift for P1 (or P2) can be understood based on the increasing capacitance C_{g1} (or C_{g2}) and inductance L_3 with t_m. Note that the extinction ratio also increases with t_m, since the transmittance for TE waves will decrease as t_m increases. Therefore, even greater extinction ratio could be obtained with the proposed structure at slightly longer wavelengths. When t_m is on the order of 100 nm (not shown in the figure), the trends for P1 and P2 are the same but the deviation of the LC circuit model from the full-wave calculation becomes large. This could be due to the different field distributions because the slit region becomes very wide and shallow. Furthermore, when the metal thickness is comparable to the penetration depth in Ag, which is on the order of 10 nm, the deviation of LC model from the full-wave calculation becomes prominent. For this case, the current will flow through the whole metallic layer and the LC circuit models must be modified to consider such effect.

Figure 3(b) shows that when the spacer thickness t_s is reduced, P1 will redshift but P2 will blueshift and they will degenerate into one peak when t_s < 20 nm. For P1, the spacer capacitance C_s increases with decreasing t_s, so that the resonance wavelength will increase. For P2, on the other hand, C_{g2} decreases with decreasing t_s due to the second term, so that the resonance wavelength will also decrease. When t_s exceeds 50 nm, the LC model predictions start to deviate from the full-wave simulation. In this case, near-field coupling between the top and bottom grating becomes weak. Furthermore, the field distributions may largely deviate from those for the base parameters, resulting in a breaking down of the LC circuit models.

#186509 - $15.00 USD Received 6 Mar 2013; revised 13 Apr 2013; accepted 14 Apr 2013; published 23 Apr 2013

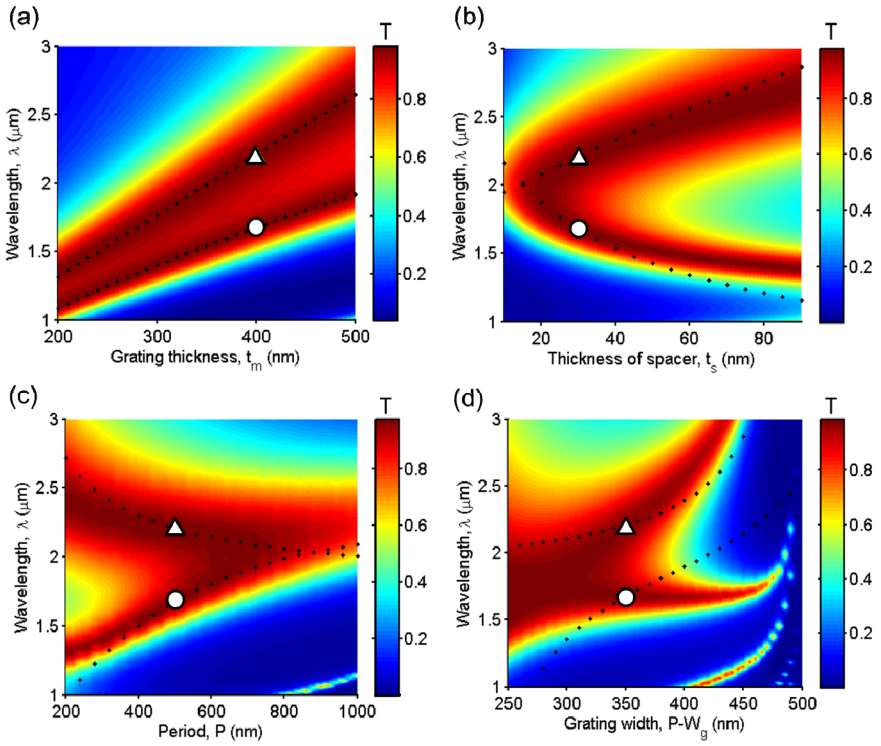

Fig. 3. The effect of certain geometric parameters on the normal transmittance for TM waves using the parameters given in Fig. 1 as the base set: (a) Ag grating thickness t_m ; (b) Spacer thickness t_s ; (c) Period P by keeping $W_g / P = 0.3$; (d) Grating strip width $P - W_g$. Note that the circle and triangle marks indicate the locations of P1 and P2, respectively, according to the base parameters.

To study the scaling effect, both the slit width W_g and the period P are changed, while their ratio is fixed to be 0.3. When the structure is scaled down, a broader high transmission region is obtained as shown in Fig. 3(c). On the other hand, the two peaks merge when $P >$ 600 nm. The LC models agree reasonably well with the full-wave results, except when the period is less than 300 nm. For very small P, the penetration depth in Ag may become comparable with the width of the ridge, so that the field for different periods may couple with each other.

The effect of slit width W_g is also examined by fixing the grating period and other parameters and the results are shown in Fig. 3(d), where the abscissa is the ridge width (P – W_g). When $P - W_g > 350$ nm, the two peaks further split and the enhancement of transmittance with reducing slit width for some wavelengths is counter-intuitive. For broadband polarizer, the performance is still good when $P - W_g = 400$ nm (i.e., with a slit width of 100 nm only). For even smaller slit width, the structure can be used as a narrow band polarizer. Blocking-enhanced transmission has been predicted in 1D double-layer gratings [8, 27] and experimentally demonstrated for a 2D periodic structure [18]. Because the LC models were developed considering the field distributions using the base parameters, large deviations occur when $P - W_g$ is far away from 350 nm. The agreement in the predicted trends suggests that the excitation of MPs is still responsible for the transmission enhancement of the two branches. However, more suitable LC circuit may need to be developed according to the field distributions. It should be noted that a weak branch appears in the wavelength range from 1 to 1.5 μm when $P - W_g > 400$ nm. This branch can be quantitatively explained with a LC model considering the coupling between the top and bottom gratings in the spacer region where the ridges overlap, although the details are not shown here.

#186509 - $15.00 USD Received 6 Mar 2013; revised 13 Apr 2013; accepted 14 Apr 2013; published 23 Apr 2013

5. Concluding remarks

A design of broadband polarizers in the near infrared region is proposed with both good transmission and extremely high extinction ratio. The good performance holds until 60°. MPs are responsible for the high transmission and two simple LC models are developed to predict resonant transmission peaks quantitatively. The geometric parameters, such as grating thickness, spacer thickness, and period could be tuned for different applications. This work will benefit the design of high-performance polarizers, beamsplitters, filters, and transparent electrodes.

Acknowledgments

This study was supported by the National Science Foundation under grant CBET-1235975 (XLL) and the Department of Energy under contract DE-FG02-06ER46343 (BZ and ZMZ).

#186509 - $15.00 USD Received 6 Mar 2013; revised 13 Apr 2013; accepted 14 Apr 2013; published 23 Apr 2013